Vietnam Journal of Science and Technology ***63*** *(3) (2025) 576-589*

doi:10.15625/2525-2518/20974

Simulation and experimental study of motorcycle engine fueled with HHO enriched gasoline

Vo Anh Vu[1], Bui Van Ga[1], Le Khac Binh[2,*], Pham Van Quang[3]

[1]*Danang University of Science and Technology, The University of Danang, 54 Nguyen Luong Bang Street, Lien Chieu District, Da Nang City, Viet Nam*

[2]*Vinh University of Technology Education, No. 117 Nguyen Viet Xuan Street, Hung Dung Ward, Vinh City, Viet Nam*

[3]*Dong A University, No. 33 Xo Viet Nghe Tinh Street, Hai Chau District, Da Nang City, Viet Nam*

[*]Email: *khacbinhktv@gmail.com*

Received: 18 June 2024; Accepted for publication: 18 September 2024

Abstract. The study presents the results of simulation and experimental research on the effects of HHO addition to gasoline motorcycle engine. The results show that adding HHO to gasoline improves combustion efficiency, resulting in increased maximum pressure. Compared to an engine fueled with neat gasoline, the brake power improvement is 3.8 %, 7.1 %, and 12.1 % when substituting 5 %, 7 %, and 10 % of gasoline with HHO, respectively. The increase in combustion temperature due to the addition HHO to gasoline results in higher NO_x concentrations in the exhaust gas. Increasing the advanced ignition angle slightly decreases CO concentration but significantly increases NO_x concentration. For engines running on gasoline supplemented with HHO, the optimal ignition advance angle is reduced by 5°CA compared to the neat gasoline fueling mode. Increasing engine speed decreases indicated engine work cycle and NO_x concentration in exhaust gases while causing a slight increase in CO concentration. The discrepancy between the output power and CO concentration provided by the simulation and the experimental results is less than 10 %.

Keywords: Renewable energy, Hydrogen, Motorcycle, HHO, SI Engine.

Classification numbers: 3.3.1, 3.4.1, 3.5.1, 5.10.1.

1. INTRODUCTION

Motorcycles serve as the primary mode of personal transportation in many countries, particularly in South East Asia. The high-speed operation of motorcycle engines often affects combustion efficiency, resulting in elevated levels of pollutant emissions. To address these challenges and enhance engine performance, supplementing gasoline with hydrogen-containing fuel, such as HHO, presents a promising solution.

HHO is a gas mixture composed of hydrogen (H_2) and oxygen (O_2) in a volumetric ratio of 2:1. This gas ignites at approximately 570 °C under atmospheric pressure and stoichiometric conditions. The ignition energy of hydrogen is very low, at only 20 μJ. HHO can be generated through water electrolysis and is typically produced on-demand for immediate engine use, thereby eliminating the need for storage. The compact design of HHO gas generators facilitates their application in vehicles or stationary engines. The HHO generation system operates in synchronization with the engine: it produces HHO when the engine is running and stops production when the engine is turned off. Due to the wide flammability limits of hydrogen, engine torque can be optimized by adjusting the equivalence ratio rather than the mixture flow rate. This characteristic makes HHO an effective additive for improving fuel efficiency and reducing emissions, especially during the low-load operations typical in urban conditions [1 - 3].

Several studies have compared the impacts of supplementing gasoline with HHO and pure hydrogen (H_2) on engine performance. The findings suggest that the gasoline-HHO mixture exhibits characteristics nearly identical to those of the gasoline-H_2 mixture and, in some cases, demonstrates even superior performance. Notably, the gasoline-HHO mixture tends to improve thermal efficiency and maintain stable combustion, particularly under lean mixture conditions [4 - 5]. Unlike H_2, HHO contains the oxygen necessary for the complete combustion of hydrogen in the fuel mixture, thereby eliminating the need for additional air supply. This intrinsic oxygen content allows engines running on a gasoline-HHO mixture to achieve higher indicated work cycles compared to those operating on a gasoline-H_2 mixture under similar conditions. Consequently, the complete combustion associated with a gasoline-HHO mixture results in lower emissions of carbon monoxide (CO) and hydrocarbons (HC) compared to the gasoline-H_2 mixture [4] .

Arjun *et al*. [6] observed that supplementing gasoline with HHO increased brake power by 2 % to 5.7 % and improved thermal efficiency from 10.26 % to 34.9 %. They also noted significant reductions in CO and HC emissions, averaging 18 % and 14 %, respectively. Similarly, Dhananjay *et al.* [7] found that in a 4-stroke spark ignition engine, HHO supplementation increased engine power by approximately 5.7 %, enhanced thermal efficiency by about 5 %, and decreased CO and HC emissions. Musmar et al. [8] conducted experiments using HHO with a Honda G200 engine and discovered that NO_x emissions decreased by approximately 50 %, CO emissions decreased by about 20 %, and fuel consumption decreased by 20 % to 30 % compared to running on gasoline alone. Rimkus *et al.* [9] similarly noted that while the indicated efficiency of engines supplemented with HHO remained relatively unchanged, there were significant reductions in CO and HC concentrations in the exhaust gas, along with soot emissions.

Contrary to these findings, Chetan et al. [10] and Kale et al. [11] reported that while CO and HC emissions decreased with HHO supplementation, NOx emissions increased. Recent studies on hydrogen supplementation into biogas have yielded similar results, showing increased indicated engine work cycles and decreased CO and HC emissions [12 - 14]. The effectiveness of HHO supplementation in biogas combustion parallels its effects in gasoline [15 - 17]. Generally, adding hydrogen or HHO to any fuel improves the combustion process. However, there are discrepancies in the trends of NO_x emissions when HHO is added to conventional fuels. Some studies suggest that NO_x levels increase with HHO supplementation in gasoline, while others indicate that NO_x concentrations decrease when the engine operates on a gasoline-HHO mixture compared to gasoline alone. The broad flammability limits of hydrogen and HHO necessitate precise control of the fuel supply system to prevent backfire during the intake process [18 - 20].

This research focuses on evaluating the effects of HHO supplementation on the performance and pollutant emissions of motorcycle engines operating under urban conditions. The aim is to exploit the regenerative energy from motorcycles operating in these conditions to produce HHO through water electrolysis and supplement it to the engine. The goal is to improve combustion efficiency during frequent low-load conditions that demand high torque. The motorcycles will be equipped with regenerative electric brakes [21], which capture electrical energy during braking, store it in a battery, and use it to electrolyze water, producing HHO for engine supply. Although the energy introduced into the engine via HHO may be relatively moderate, it is expected to significantly enhance the combustion process.

2. MATERIALS AND METHODS

2.1. Simulation

In this study, the simulation was carried out on a Honda Wave RSX FI 110cc motorcycle engine. The primary technical specifications of the engine are detailed in Table 1.

Table 1. Technical Specifications of the Honda Wave RSX FI 110 Engine.

Bore (mm)	50
Stroke (mm)	55.6
Cylinder capacity (cm^3)	109.2
Compression ratio	9.3:1
Maximum power (kW) at speed (rpm)	6.46/7500

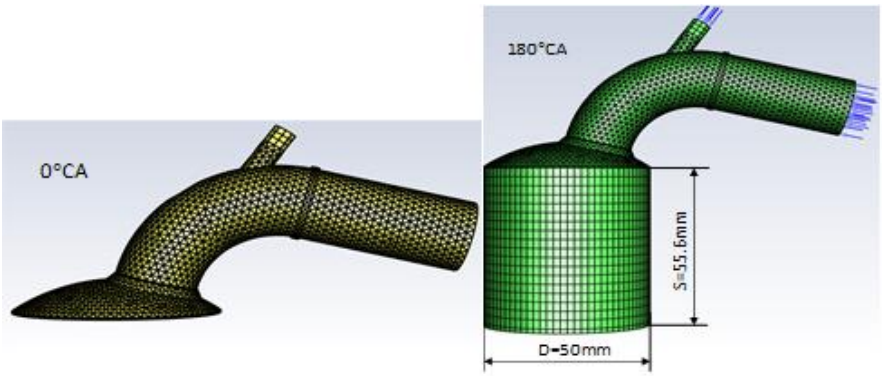

Figure 1. 3D computational space model.

The computational space of the engine includes the cylinder, combustion chamber, and intake manifold, as illustrated in Figure 1. The gasoline injection system remains unchanged from its standard configuration, while HHO is supplied through an additional injector installed upstream of the fuel injector.

A dynamic mesh was employed in the cylinder space to accommodate the changing volume during the engine cycle, while fixed grids were assigned to the remaining spaces. To optimize

computational efficiency, the intake manifold space is deactivated after closing the intake valve. Input parameters for the simulation include the pressure and temperature of the air entering the intake manifold and the pressure, temperature, and composition of the HHO. In the research the content of HHO in the mixture with gasoline is determined via the equivalence ratio of hydrogen ϕ_HThe global equivalence ratio of fuel-air mixture is defined by ϕ If the equivalence ratio of gasoline is ϕ_G, then $\phi = \phi_H + \phi_G$. Thus, ϕ_H indicates the ratio of gasoline substituted by HHO in stoichiometric mixture ϕ=1.

The computations start at the beginning of the intake process and continue until the start of the exhaust process. The engine simulation follows the ideal cycle assumption, presuming that processes initiate and conclude at the top dead center (TDC) and bottom dead center (BDC). The turbulent flow within the gas mixture is simulated using the k-ε model [25]. The formation of major species in the combustion products is modeled based on thermochemical equilibrium, while NO_x concentration is computed via reaction kinetics.

HHO consists of 2/3 hydrogen (H_2) and 1/3 oxygen (O_2) by volume. The HHO content in the fuel is quantified as the volume ratio of HHO to the total volume of the HHO-gasoline mixture. Hydrogen's high adiabatic combustion temperature and rapid burning rate enable it to combust with very lean mixtures. Despite its lower calorific value of 10.8 MJ/m³ compared to methane's 35.8 MJ/m³, hydrogen requires only 0.5 m³ of oxygen to combust completely for each cubic meter of hydrogen under standard conditions. Consequently, hydrogen occupies more volume than gasoline vapor in the same cylinder volume, but due to its lower calorific value, the energy introduced to the engine does not significantly increase compared to gasoline. The establishment of the model has been presented in the previous works [15 - 16, 23 - 24].

HHO provides sufficient oxygen to fully combust the hydrogen present, necessitating only minimal additional air to burn the gasoline. In a given cylinder volume, the oxygen required for hydrogen combustion is not derived from the air, hence there is no accompanying inert nitrogen (N_2). This increases the total fuel quantity supplied to the engine, enhancing the energy content of the fuel mixture entering the engine.

The simulations were executed using ANSYS Fluent 2021R1. The combustion process was simulated using a partially premixed combustion model. The combustion model outputs include the composition of species in the combustion mixture, such as CO, under thermochemical equilibrium conditions. The NO_x formation rate is calculated according to the Zeldovitch mechanism. In this work the global equivalence ratio is fixed at stoichiometric value (ϕ = 1). Performance and emissions of the engine were considered under effects of HHO concentration, advanced ignition angle and engine speed.

2.2. HHO gas generator

A dry-type HHO gas generator (Figure 2) was selected due to its superior efficiency and minimal heat generation compared to wet-type generators. These generators are compact and suitable for integration into motorcycles, offering low maintenance costs due to their corrosion-resistant stainless steel electrodes.

The design parameters were carefully chosen to optimize gas production while considering practical limitations. The electrode plates were set at an optimal distance of 3mm to facilitate efficient gas bubble release. Each plate, sized at 120x120mm, was cross-roughened on both sides to maximize surface area, enhancing bubble formation and detachment efficiency. This surface treatment was followed by immersion in an electrolyte solution for three days to create a protective coating that aids in electrolysis.

To achieve efficient water electrolysis, the gas generator was configured with 8 compartments containing 9 plates: 2 negative electrodes on the outer sides, 1 positive electrode in the middle, and 6 intermediate plates between them. The voltage across each cell was controlled using a PWM pulse width regulator, maintaining an applied voltage of 1.5 - 2V, optimized for electrolysis efficiency.

Experiments confirmed that NaOH was chosen as the electrolyte due to its effectiveness in water splitting, despite its tendency to corrode electrodes. An 18% concentration of NaOH in water was found suitable for accelerating the electrolytic reaction, minimizing energy consumption.

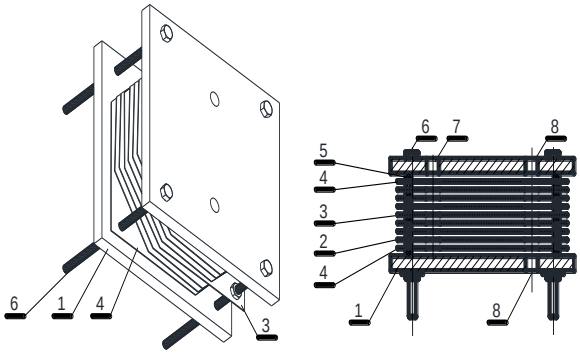

Figure 2. Structure of HHO Gas Generator. 1-Flange; 2-Intermediate electrode plate; 3-Positive electrode plate; 4-Negative electrode plate; 5-Rubber cushion; 6-Fixing screw; 7-Electrolyte solution inlet; 8-HHO gas output

The HHO supply system (Figure 3) includes the HHO gas generator powered by the motorcycle's 12V-60Ah battery. An 18 % NaOH electrolyte solution tank supplies the generator through dedicated pipes. The produced HHO gas is transferred to an HHO tank before being delivered to the engine through an air pipe connected to the HHO outlet.

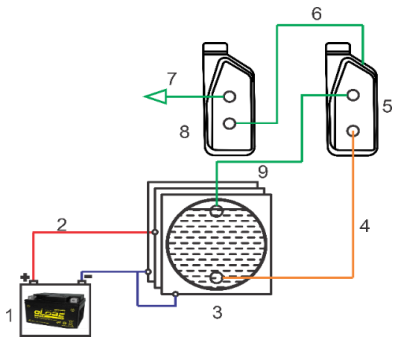

Figure 3. Diagram of the HHO Gas Generation System. 1. Battery, 2. Power supply to HHO generator, 3. HHO generator, 4. Electrolyte supply, 5. Electrolyte tank, 6. HHO conducting tube, 7. HHO gas, 8. Flashback arrestor.

Figure 4. Installation of Dry-Type HHO Gas Generator into motorcycle.

2.3. Experimental equipment

The engine power is measured by the Supper Dyno L50 (Figure 5a). This instrument measures the power at the traction wheel of the vehicle up to 25 HP at maximum vehicle speed of 110 km/h and maximum engine speed of 16000 rpm. The engine power is then calculated via the mechanical efficiency of the system [22]. This study used the gas analyzer Opus 400 to analyze exhaust gases (Figure 5b). It can measure CO (0 - 15 vol.%), HC (0 – 15000 ppm vol. ppm), and NO_x (0-5000 vol. ppm).

Figure 5: Experimental instruments: (a) Super Dyno L50, (b) Gas analyzer Opus 400

3. RESULT AND DISCUSSION

3.1. Effects of HHO content on combustion

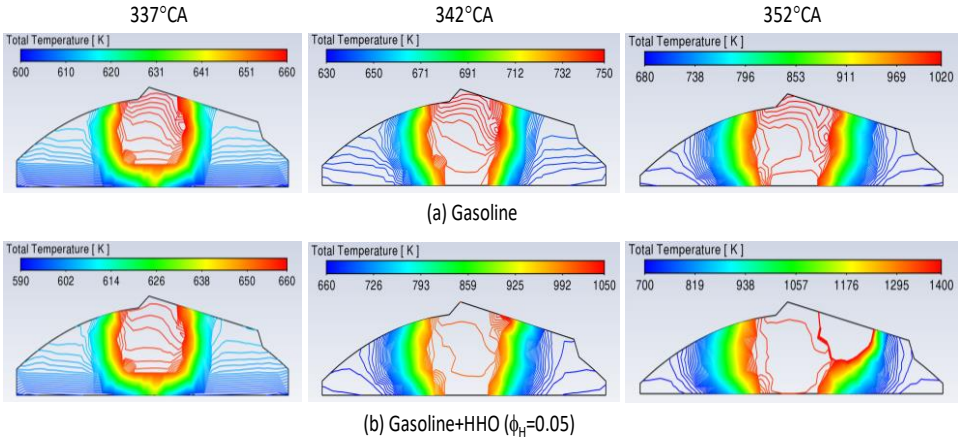

Figure 5. Comparison of flame front development when the engine was fueled with gasoline and with gasoline+HHO (ϕ_H = 0.05, ϕ = 1, φ_s = 25 °CA, n = 7500 rpm).

Figure 6 compares the development of flame front when the engine was fueled with pure gasoline and with gasoline supplemented by HHO (ϕ_H = 0.05). This comparison is made at an equivalence ratio global ϕ = 1, in which the equivalence ratio contributed by HHO is ϕ_H = 0.05. The engine operates at speed of 7500 rpm, and a fixed ignition angle at 135 °CA (Advanced ignition angle φ_s = 25°CA. It is observed that at the same crankshaft angle, the maximum temperature of the combustion products increases when HHO is added to gasoline. Furthermore,

the addition of HHO to gasoline increases the flame speed, resulting in a larger volume of the burned mixture than the gasoline fueling mode.

Figure 7a illustrates the variation in cylinder pressure with respect to the crankshaft angle when the engine runs on pure gasoline and on gasoline supplemented by HHO with different composition. This comparison is made under conditions of the global equivalence ratio ϕ=1, the composition of HHO is expressed through its equivalence ratio ϕ_H. The engine operates at speed of 7500 rpm, and a fixed ignition advance angle of φ_s = 22 °CA.

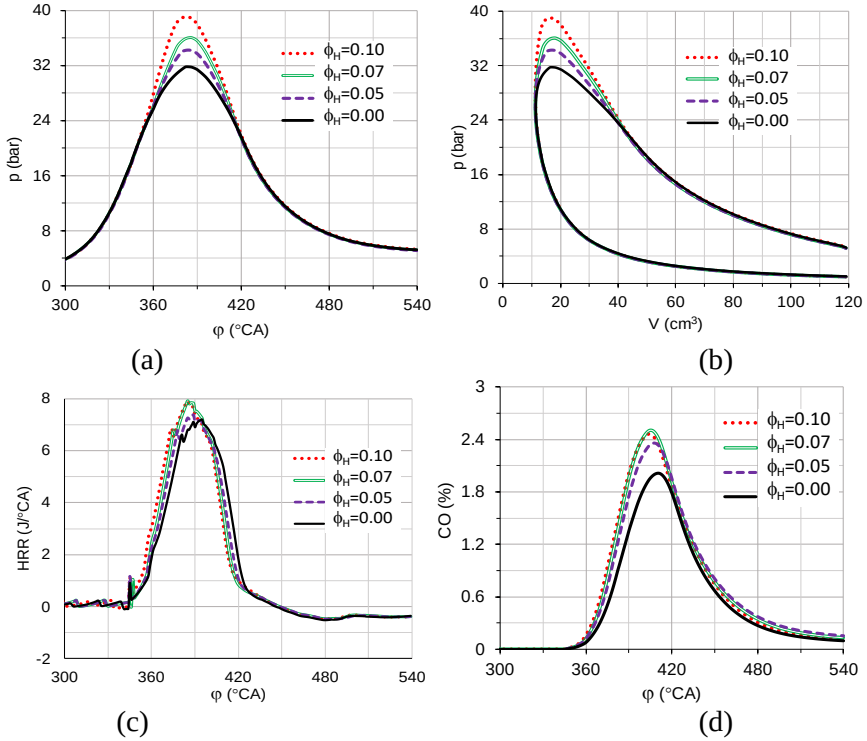

Figure 7. Effect of HHO on variations of pressure (a) work diagram (b) heat release rate (c) and CO concentration (d) according to crankshaft angle (n = 7500 rpm, ϕ = 1, φ_s = 22 ^{o}CA).

We observe that with the addition of HHO to gasoline, the maximum pressure in the cylinder increases and the peak of heat release rate (HRR) occurred earlier (Figure 7c). This can be attributed to the increased burning speed provided by the HHO, which causes the peak pressure to occur closer to TDC. Additionally, the faster burning speed results in more complete combustion, thereby enhancing thermal efficiency. Under the same operating conditions, the maximum cylinder pressure increases by approximately 7 bar when ϕ_H = 0.1 (i.e.10 % gasoline is substituted by HHO). However, because this higher pressure occurs closer to TDC, the work lost during the compression cycle increases, and as a result, the indicated work of the cycle does not increase proportionally to the maximum pressure (Figure 7b). The results show that the brake power of the engine is 6.71 kW, 6.92 kW and 7.24 kW when gasoline is substituted by 5 %, 7 % and 10 % HHO, respectively. As compared to brake power when the engine is fueled by neat gasoline (6.46 kW), the improvement of brake power is 3.8 %, 7.1 % and 12.1 % as substituting 5 %, 7 % and 10 % gasoline by HHO, respectively.

The concentrations of CO are determined using chemical equilibrium calculations of the hydrocarbon fuel combustion reaction system. Figure 7d demonstrates that when HHO content

increases, the peak value of the CO curve increases and shifts toward TDC, but the concentration of CO in the exhaust gas remains nearly unchanged compared to gasoline alone.

Figure 8a shows the effects of HHO content on the variation in the combustion temperature. Due to the increased combustion rate when blending HHO with gasoline, the temperature begins to rise earlier, and the maximum temperature point is reached closer to TDC. The increased heat release rate and combustion temperature are the main causes of the elevated concentration of NO_x in exhaust gases, according to the Zeldovich mechanism. Figure 8b illustrates the effect of adding HHO to the fuel mixture on NO_x concentration in the combustion mixture. The results indicate that under identical operating conditions and a fixed spark advance angle, NO_x concentration increases by approximately 17 %, 67 % and 140 % when substituting 5 %, 7 % and 10 % gasoline by HHO, respectively.

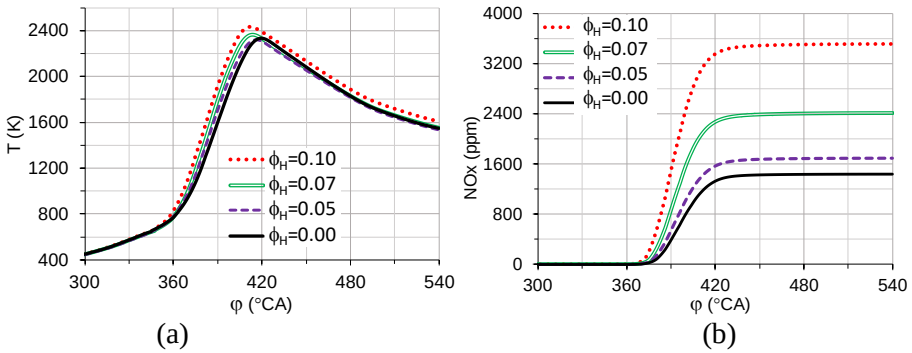

Figure 8. Effect of HHO on the variation of combustion temperature (a) and NO_x concentration (b) according to crankshaft angle (n = 7500 rpm, ϕ = 1, φ_s = 20 ^oCA).

3.2. Effects of advanced ignition angle

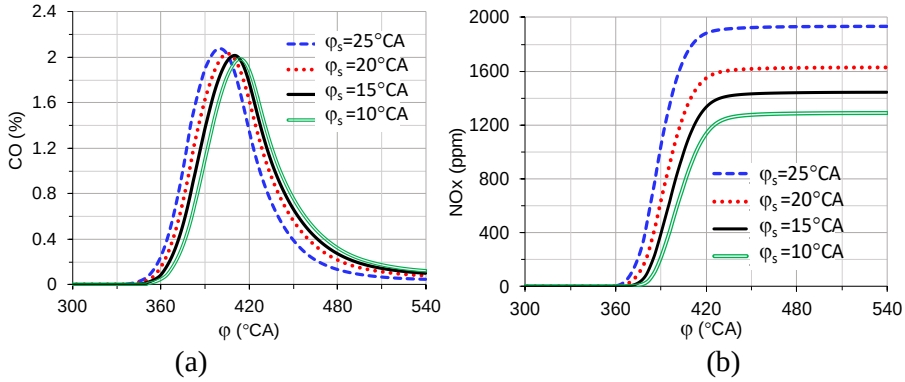

Figure 9. Effect of advanced ignition angle on the variation of CO (a), NO_x (b) concentrations according to crankshaft angle when the engine is fueled with gasoline (n = 7500 rpm, ϕ = 1).

The research results above indicate that HHO influences the combustion process and emission pollutants through its impact on burning speed. Therefore, to ensure efficient engine operation when HHO is added to gasoline, it is necessary to decrease the ignition advance angle. Figures 9a and 9b depict the influence of ignition advance angle on CO and NO_x variations in a gasoline engine operating at 7500 rpm with ϕ = 1. It is observed that increasing the ignition

advance angle shifts the peak of the CO curve towards TDC, resulting in an increase in maximum CO concentration but a slight decrease in its exhaust gas concentration. This phenomenon occurs because higher ignition advance angles elevate the combustion mixture temperature, thereby accelerating CO production. However, the increased temperature also intensifies the combustion rate of CO, leading to reduced concentration in the exhaust gas.

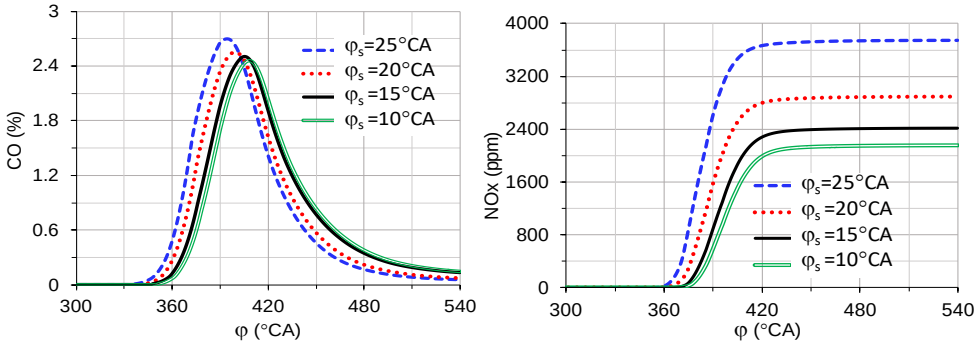

Figure 10. Effect of ignition advance angle on the variation of CO (a), NO_x (b) concentrations according to crankshaft angle when the engine is fueled with gasoline supplemented with ϕ_H = 0.07 (n = 7500 rpm, ϕ = 1).

In contrast, NO_x concentration is highly dependent on temperature. Thus, increasing the ignition advance angle leads to an increase in NO_x concentration. Figure 9b demonstrates that NO_x concentration increases by 45 % as the advanced ignition angle increases from 10 °CA to 25 °CA.

The effect of ignition advance angle on the variation of CO and NO_x concentrations with respect to crankshaft angle in case of gasoline enriched by HHO. Figure 10a shows that the concentration of CO in exhaust gas of engine is practically unchanged as shifting from gasoline fueling mode to gasoling-HHO fueling mode. However, the NO_x concentration is approximately double when adding HHO to gasoline as the engine operates under the same conditions.

3.3. Comparison simulation and experiment in full loading regime

In this section, we compare the variations in brake power, CO and NO_x concentrations in exhaust gases according to engine speed at full loading regime through simulation and experimental data analysis. The advanced ignition angle varies from 15 °CA to 20 °CA when the engine speed varies from 4500 rpm to 7500 rpm. Figure 11a illustrates that the peak pressure decreases when increasing the engines speed. This is due to the decrease in volumetric efficiency and incomplete combustion. The peak of combustion temperature is practically unchanged, but the temperature in the exhaust gas increases with engine speed because the combustion is extended in the expansion stroke (Figure 11b). As engine speed increases, the CO concentration in the exhaust gas increases due to incomplete combustion (Figure 11c).

Figure 11d depicts the effect of engine speed on the variation of NO_x concentration concerning crankshaft angle. It is evident that as engine speed increases, NO_x concentration decreases. This phenomenon occurs because the existing time of combustion mixture in a high-temperature medium decreases as engine speed increases. This shortens the time for NO_x formation.

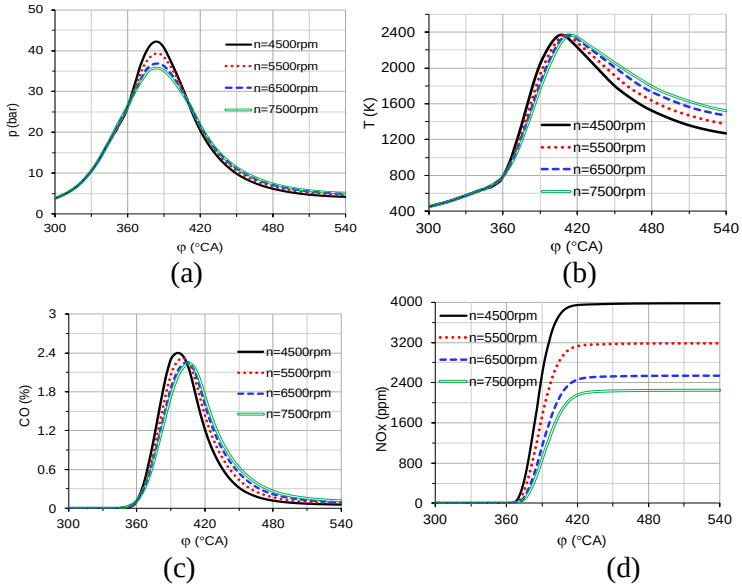

Figure 11. Effect of engine speed on the variation of in-cylinder pressure (a), combustion temperature (b), CO concentration (c) and NO_x concentration (d) with respect to crankshaft angle when the engine is fueled with gasoline substituted by 2 % HHO (ϕ = 1, φ_s variable).

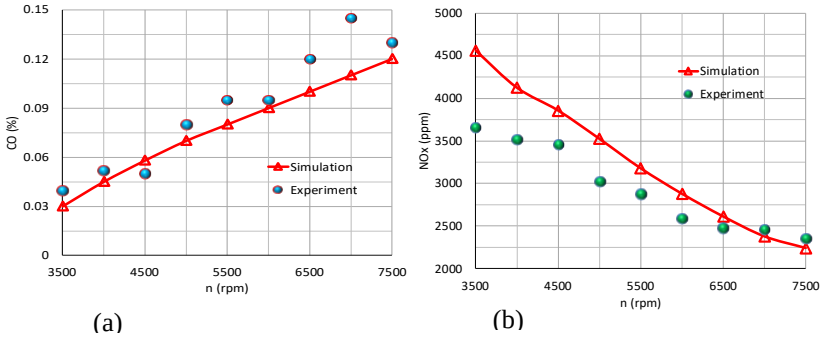

Figure 12. Comparison of simulation and experimental data on the variation in CO (a) and NO_x (b) concentrations with respect to engine speed when the engine is fueled with gasoline substituted by 2 % HHO (ϕ = 1, φ_s variable).

Figure 12a compares the variation of CO concentration with engine speed when running on gasoline substituted by 2 % HHO, with ϕ = 1 and φ_s variable. It shows that CO concentration increases with engine speed. The CO concentration given by experiment is higher than simulation results. This can be attributed by the fact that the combustion in real combustion chamber is less complete than that in simulation. The difference between simulation and measurement becomes larger at high engine speed. This is because the incomplete combustion becomes more significantly at high engine speed. The everage difference between simulation and experiment in CO concentration is by 8 %.

Figure 12b compares the variation of NO_x concentration with engine speed given by simulation and experiment. It reveals that experimental NO_x concentrations are generally lower across most speed ranges than simulated values. This difference can be attributed to the actual

combustion temperatures being lower than the calculated value due to less ideal combustion processes in practice. The difference of NO_x concentration given by simulation and experiment is more significant in the low engine speed region. This may be because the NO_x formation rate in practice is lower than in simulation.

Power used for comparison in this study refers to the output power at the engine crankshaft. The simulation results provide the indicated power (P_i). Thus, the power obtained at the crankshaft output is calculated using the mechanical efficiency of the engine, $P_e = \eta_{engine} \cdot P_i$. The experimental power (P_w) measured by the engine dynamometer is the power at the wheel. Therefore, the power at the crankshaft output can be expressed as $P_e = P_w/\eta_{dyno}$. For the motorcycle's drivetrain and engine system, the mechanical efficiency of engine and dyno can be chosen generally as $\eta_{engine} = 0.85$ and $\eta_{dyno} = 0.65$. The average power obtained from five experimental measurements at engine speeds of 4000, 5000, 6000, and 7000 rpm is compared with the simulation results. It is observed that the discrepancy between the crankshaft output power provided by the simulation and the experimental results is less than 10 % (Figure 13). This result indicates a good agreement between simulation and experimental outcomes. It confirms the reliability of the comparative performance results of the engine running on gasoline and on HHO-enriched gasoline as provided by the simulation.

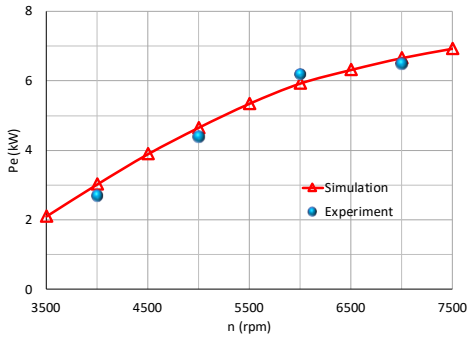

Figure 13. Comparison of simulation and experimental data on the variation of brake power with respect to engine speed when the engine is fueled with gasoline substituted by 2 % HHO ($\phi = 1$, φ_s variable)

4. CONCLUSIONS

Based on the above research results, the following conclusions can be drawn:

- Adding HHO to gasoline improves combustion efficiency, resulting in increased maximum pressure. Compared to an engine fueled with neat gasoline, the brake power improvement is 3.8 %, 7.1 %, and 12.1 % when substituting 5 %, 7 %, and 10 % of gasoline with HHO, respectively.
- The increase in combustion temperature due to the addition of HHO to gasoline results in higher NO_x concentrations in the exhaust gas. Specifically, NOx concentrations increase by approximately 17 %, 67 %, and 140 % when substituting 5 %, 7 %, and 10 % of gasoline with HHO, respectively, compared to the gasoline fueling mode.
- Increasing the advanced ignition angle slightly decreases CO concentration but significantly increases NOx concentration. For engines running on gasoline supplemented

with HHO, the optimal ignition advance angle is reduced by 5 °CA compared to the neat gasoline fueling mode.

- Increasing engine speed decreases indicated engine cycle work and NOx concentration in exhaust gases while causing a slight increase in CO concentration. The discrepancy between the output power and CO concentration provided by the simulation and the experimental results is less than 10 %.

Acknowledgement: This work was supported by The University of Danang, University of Science and Technology, under Project code T2024-02-04.

CRediT authorship contribution statement. Vo Anh Vu: Methodology, Investigation. Bui Van Ga: Formal analysis, Funding acquisition. Le Khac Binh: Formal analysis, Supervision. Pham Van Quang: Formal analysis.

Declaration of competing interest. The authors declare that they have no known competing financial interests or personal relationships that could have appeared to influence the work reported in this paper.

REFERENCES

1. Rajasekaran T., Duraiswamy K., Bharathiraja M. *et al*. - Characteristics of engine at various speed conditions by mixing of HHO with gasoline and LPG, ARPN Journal of Engineering and Applied Sciences **10** (1) (2015) 46-51.
2. Changwei Ji and Wang, S. - Combustion and emissions performance of a hybrid hydrogen-gasoline engine at idle and lean conditions, International Journal of Hydrogen Energy **35** (1) (2010) 346-355. https://doi.org/10.1016/j.ijhydene.2009.10.074
3. Wang S., Ji C., B. Zhang, Liu X. - Realizing the part load control of a hydrogen-blended gasoline engine at the wideopen throttle condition, Int. J. Hydrogen Energy **39** (14) (2014) 7428-7436. https://doi.org/10.1016/j.ijhydene.2014.03.024
4. Wang S., Ji C., Zhang J., Zhang B. - Comparison of the performance of a spark-ignited gasoline engine blended with hydrogen and hydrogen-oxygen mixtures, Energy **36** (10) (2011) 5832-5837. https://doi.org/10.1016/j.energy.2011.08.042
5. S. Wang, C. Ji, J. Zhang, B. Zhang - Improving the performance of a gasoline engine with the addition of hydrogen-oxygen mixtures, Int. J. Hydrogen Energy **36** (17) (2011) 11164-11173. https://doi.org/10.1016/j.ijhydene.2011.05.138
6. T. B. Arjun, K. P.Atul, P. Ajay, *et al*. - A review on analysis of HHO gas in IC engines, Materials Today Proceedings, Vol. 11, Part 3, 2019, pp. 1117-1129. https://doi.org/ 10.1016/j.matpr.2018.12.046
7. Dhananjay Babariya, Jay Oza, Bhavin Hirani, *et al*. - An Experimental Analysis of S.I Engine Performance with HHO as a Fuel, International Journal of Research in Engineering and Technology (IJRET4) (4) (2015) 608-614.
8. Sa'ed A. Musmar, Ammar A. Al-Rousan - Effect of HHO gas on combustion emissions in gasoline engines, Fuel **90** (10) (2011) 3066-3070. https://doi.org/10.1016/j.fuel. 2011.05.013
9. Alfredas Rimkus, Jonas Matijošius, Marijonas Bogdevičius, *et al*. - An investigation of the efficiency of using O_2 and H_2 (hydrooxile gas-HHO) gas additives in a CI engine operating on diesel fuel and biodiesel, Energy **152** (2018) 640-651. https://doi.org/ 10.1016/j.energy.2018.03.087

10. Chetan N. Patel, Prof. Maulik A. Modi, Dr. Tushar M. Patel - An Experimental Analysis of IC Engine by Using Hydrogen Blend, International Journal of Recent Trends in Engineering & Research (IJRTER) **2** (4) (2016) 453-462.
11. K. A. Kale and M. R. Dahake - The Effect of HHO and Biodiesel Blends on Performance and Emission of Diesel Engine-A Review, International Journal of Current Engineering and Technology (5) (2016) 1-9. http://doi.org/10.14741/Ijcet/22774106/spl.5.6.2016.1
12. Ga V. B., Dong V. D., Tan V. B., Trung Q. N. - Effect of H2 Composition to Performance and Pollution Emission of Hydrogen Enriched Biogas Diesel Dual Fuel Engine, The 20th Vietnam Fluid Mechanics Association, Can Tho, July 27-29, 2017, pp. 238-245.
13. Ga V. B., Nam V. T., Tu M. T. B., Trung Q. N. - Numerical simulation studies on performance, soot and NOx emissions of dual-fuel engine fuelled with hydrogen enriched biogas mixtures, IET Renewable Power Generation **12** (10) (2018) 1111-1118, DOI: 10.1049/iet-rpg.2017.0559
14. Ga V. B., Tuan X. C., Thai. P. Q., Tien M. Le, Dong V. N. - Effect of hydrogen enriched biogas on indicated engine cycle work and NOx emission of SI engine. The 21st Vietnam Fluid Mechanics Association, Qui nhon 19-21/7/2018, pp. 175-184
15. Ga V. B, Tu M. T. B., Tram B. L. T., Tung N. V., Huy X. D., - Combustion Improvement of Engine Fueled With Poor Biogas By Blending Hydroxyl (HHO), The University of Danang, Journal of Science and Technology **17** (1) (2019) 35-41
16. Ga V. B., Tung. H. T. T., Tien M. Le., Tu M. T. B., Nghia V. D., Sang T. N. T., Performance and pollution emissions of a biogas-HHO port injection engine, The University of Danang, Journal of Science and Technology **18** (1) (2020) 43-48.
17. Ga V. B, Tu M. T. B, Dong V. N., Hung V. B. - Analysis of combustion and NOx formation in a SI engine fueled with HHO enriched biogas, Environmental Engineering and Management Journal **19** (5) (2020) 317-327.
18. Nam V. T., Ga V. B., Duc V. P., Tu M. T. B. - Supply the biogas-hydrogen fuel for spark ignition engine drag the electric generator in the hybrid of renewable energy system, The 21st Vietnam Fluid Mechanics Association, Quy Nhon, 19-21/7/2018, pp. 448-458
19. Ga V. B., Tu M. T. B., Tram B. L. T., Hung V. B. - Technique of Biogas-HHO Gas Supply for SI Engine, International Journal of Engineering Research & Technology (IJERT) **8** (5) (2019) 669-674
20. Ga V. B., Vu A. V., Tu M. T. B., Hung V. B., Tram B. L. T., Quang V. P. - Air/fuel ratio control of a SI-engine fueled with poor Biogas-HHO, The University of Danang, Journal of Science and Technology **17** (3) (2019).
21. Tung. H. T. T., Ga V. B., Vu A. V., Tan V. B. - Eco motorcycle, The 21st Vietnam Fluid Mechanics Association, Quy Nhon 19-21/7/2018, pp. 894-906
22. M. Durack - Making sense of two-wheeler fuel efficiencies, Auto Tech Review, Vol. 5, 10/01 2016, pp. 20-25, , doi: https://doi.org/10.1365/s40112-016-1215-7
23. Ga V. B., Tu M. T. B,. Nam V. T., Huang Z., Hoang A. T., Wieslaw T, Hung V. B., Mai X. P., Phuoc Q. P. N. - Flexible syngas-biogas-hydrogen fueling spark-ignition engine behaviors with optimized fuel compositions and control parameters, International Journal of Hydrogen Energy. Available online 7 October 2022, https://doi.org/10.1016/j.ijhydene.2022.09.133
24. Thanh L. C. N., Ga V. B., Tuy V. L., Dong V. N**. -** Motorcycle Engine Fueled with Gasoline Enriched by HHO Produced with Regenerative Braking Energy MMMS2022,

pp361-368, Lecture Notes in Mechanical Engineering 2024 ISSN 2195-4364 (electronic), ISBN 978-3-031-39090-6 (eBook). https://doi.org/10.1007/978-3-031-39090-6

25. Ga V. B., Nam V. T, Dong V. N., Trung Q. N., Tien T. H. - Octane number stratified mixture preparation by gasoline–ethanol dual injection in SI engines, International Journal of Environmental Science and Technology **16** (7) (2018) 3021-3034. https://doi.org/10.1007/s13762-018-1942-1